Available online at www.sciencedirect.com
ScienceDirect
Journal of Nuclear Materials 356 (2006) 256–263
journal of nuclear materials
www.elsevier.com/locate/jnucmat

Tensile tests and TEM investigations on LiSoR-2 to -4

Y. Dai *, B. Long, X. Jia, H. Glasbrenner, K. Samec, F. Groeschel

Spallation Neutron Source Division, Paul Scherrer Institut, CH-5232 Villigen PSI, Switzerland

Abstract

Martensitic steel T91 will be used for the liquid lead bismuth eutectic (LBE) container of the MEGAPIE target. The irradiation assisted LBE corrosion and embrittlement effects on the behaviours of T91 steel have been studied by performing the LiSoR experiments, where T91 steel was irradiated with 72 MeV protons to doses up to 0.2 dpa at temperatures above 300 °C in flowing LBE with or without mechanical stress. Tensile tests on the T91 steel after irradiation demonstrated that the irradiation assisted LBE embrittlement was not evident at such a low irradiation dose. The irradiation produced small defect clusters and dislocation loops were observed in the inner tensile-stressed specimens (ITS-specimens) of LiSoR-3 and LiSoR-4. The main features of the dislocation structure in the ITS-specimen of LiSoR-2 and the test-section tubes (TS-tubes) were dislocation tangles and dislocation networks, and small defect clusters and dislocation loops were hardly observed due to the high irradiation temperatures. The TEM observations support the results of the tensile tests.

1. Introduction

In the MEGAPIE (megawatt pilot target experiment) target [1], martensitic steel T91 is selected as the material for the liquid lead bismuth eutectic (LBE) container. The degradation of the mechanical properties of the T91 steel in the proton beam entrance window of the LBE container is one of key parameters limiting the lifetime of the target. In order to investigate the behaviours of the T91 steel in the beam window, LiSoR (liquid–solid reaction under irradiation) experiments were performed by installing a LBE loop at the Injector-I at the Paul Scherrer Institut (PSI), Switzerland, in which the T91 steel was irradiated with 72 MeV protons at temperatures above 300 °C in flowing LBE with or without mechanical stress [2].

Four LiSoR experiments were conducted. Among them, the second experiment (LiSoR-2) was terminated when a leak of LBE was detected. The leak located in the irradiation zone of the test-section-tube (TS-tube) [3]. The third and fourth experiments (LiSoR-3 and -4) were also ended earlier than as planned due to some unexpected incidences. Nevertheless, no evident damage was observed in the TS-tubes of LiSoR-3 of and LiSoR-4 after irradiation. The maximum irradiation dose for the LiSoR-2 was about 0.1 dpa, and 0.2 dpa for both LiSoR-3 and -4.

Post-irradiation examinations have been conducted on both TS-tubes and inner-tensile-stressed-specimens (ITS-specimens) of LiSoR-2 to -4. The optical microscopy, scanning electron microscopy (SEM) and transmission electron microscopy

* Corresponding author. Tel.: +41 56 310 4171; fax: +41 56 310 4529.
E-mail address: yong.dai@psi.ch (Y. Dai).

0022-3115/$ - see front matter
doi:10.1016/j.jnucmat.2006.05.010

(TEM) performed on LiSoR-2 demonstrated that a crack formed in the irradiation zone of the tube which was introduced by thermal fatigue at high temperature caused by an over-focused beam [4]. In the material in the irradiation zones of both the TS-tube and the ITS-specimen dislocation cell structure was well developed, which indicated heavy deformation due to thermal fatigue. An oxide layer of a few microns was formed on the surface in the irradiation zone of the ITS-specimen [4]. The surface analysis results of LiSoR-3 are reported elsewhere in the same proceedings [5]. In the present paper, results on the changes in the mechanical properties and microstructure of LiSoR-2 to -4 will be described.

2. Experimental

The materials used for the TS-tube and ITS-specimen are type T91 martensitic steel but with a slightly different composition. The T91 steel for the TS-tube was produced by the Creusot Loire Industrie (France) with a composition in wt% of 8.26 Cr, 0.13 Ni, 0.95 Mo, 0.43 Si, 0.38 Mn, 0.1 C, 0.2 V, 0.017 P, 0.065 Nb and with Fe in balance. While the T91 steel used for the ITS-specimen was obtained from the Ugine (France) with a composition in wt% of 8.63 Cr, 0.23 Ni, 0.95 Mo, 0.31 Si, 0.43 Mn, 0.1 C, 0.21 V, 0.02 P, 0.09 Nb and with Fe in balance. Both materials had a heat treatment: normalized at 1040 °C for 1 h followed by air cooling, and then tempered at 760 °C for 1 h followed by air cooling.

The detailed information of LiSoR experiments was presented in [2–5]. Therefore, in this paper only a brief summary is given as listed in Table 1. It is necessary to point out that the small and wobbling proton beam spot together with the cooling of flowing LBE induced a very complex temperature and stress distribution in the irradiation area, which changed with the proton beam at the same frequency of f_y, namely 1.16 Hz in LiSoR-2 and

Table 1
Materials and irradiation conditions of the TS-tubes and ITS-specimens of LiSoR-2 to -4

Parameter		LiSoR-2	LiSoR-3	LiSoR-4
Irradiation duration		34 h	264 h	144 h
Proton beam current		49 μA	15 μA	30 μA
Beam geometry		$\sigma_x = \sigma_y = 0.8$ mm	$\sigma_x = \sigma_y = 1.6$ mm	$\sigma_x = \sigma_y = 1.2$ mm
Beam wobbling frequency		$f_x = 14.3$ Hz $f_y = 1.16$ Hz	$f_x = 14.3$ Hz $f_y = 2.38$ Hz	$f_x = 14.3$ Hz $f_y = 2.38$ Hz
Averaged proton energy[a]	TS-tube ITS-specimen	70 MeV 40 MeV	70 MeV 40 MeV	70 MeV 40 MeV
Peak oscillating temperature LBE-surface[b]	TS-tube ITS-specimen	480 °C 430 °C	335 °C 325 °C	400 °C 375 °C
Peak oscillating temperature maximum[c]	TS-tube ITS-specimen	760 °C 520 °C	385 °C 340 °C	550 °C 420 °C
Maximum stress[d]	TS-tube ITS-specimen	180 MPa 200 MPa	25 MPa 200 MPa	75 MPa 200 MPa
Irradiation dose[e]	TS-tube ITS-specimen	0.1 0.075	0.2 0.15	0.2 0.15
He concentration[f]	TS-tube ITS-specimen	3.6 appm 2.6 appm	7.2 appm 5.2 appm	7.2 appm 5.2 appm

[a] Shown in Fig. 8 of [2].
[b] Temperature at the LBE-contacting surface, which oscillated with the wobbling beam spot. The values are extrapolated from the calculation of LiSoR-5 [6].
[c] The maximum temperature in the ITS-specimen was in the central position but at the out surface of the TS-tube. The values are also extrapolated from the calculation of LiSoR-5 [6].
[d] For the TS-tubes the values are for the maximum shear stress. For ITS-specimens they are the tension stress mechanically applied [2]. At the same time, the localized compression stress is about six times of the shear stress.
[e] Shown in Figs. 10 and 11 of [2].
[f] The helium concentration of LiSoR-2 was measured [7]. The others were calculated using LiSoR-2 data.

2.38 Hz in LiSoR-3 and -4 [6]. The localized high temperature spot generated a large temperature gradient not only in the transversal direction but also in longitudinal direction, which resulted in significant thermal stresses inside the irradiation zones of both the TS-tube and ITS-specimen. The largest component of the thermal stress was in compression, which was about six times of the shear stress. In an ITS-specimen, the compression stress reduced the mechanically applied tension stress. As a

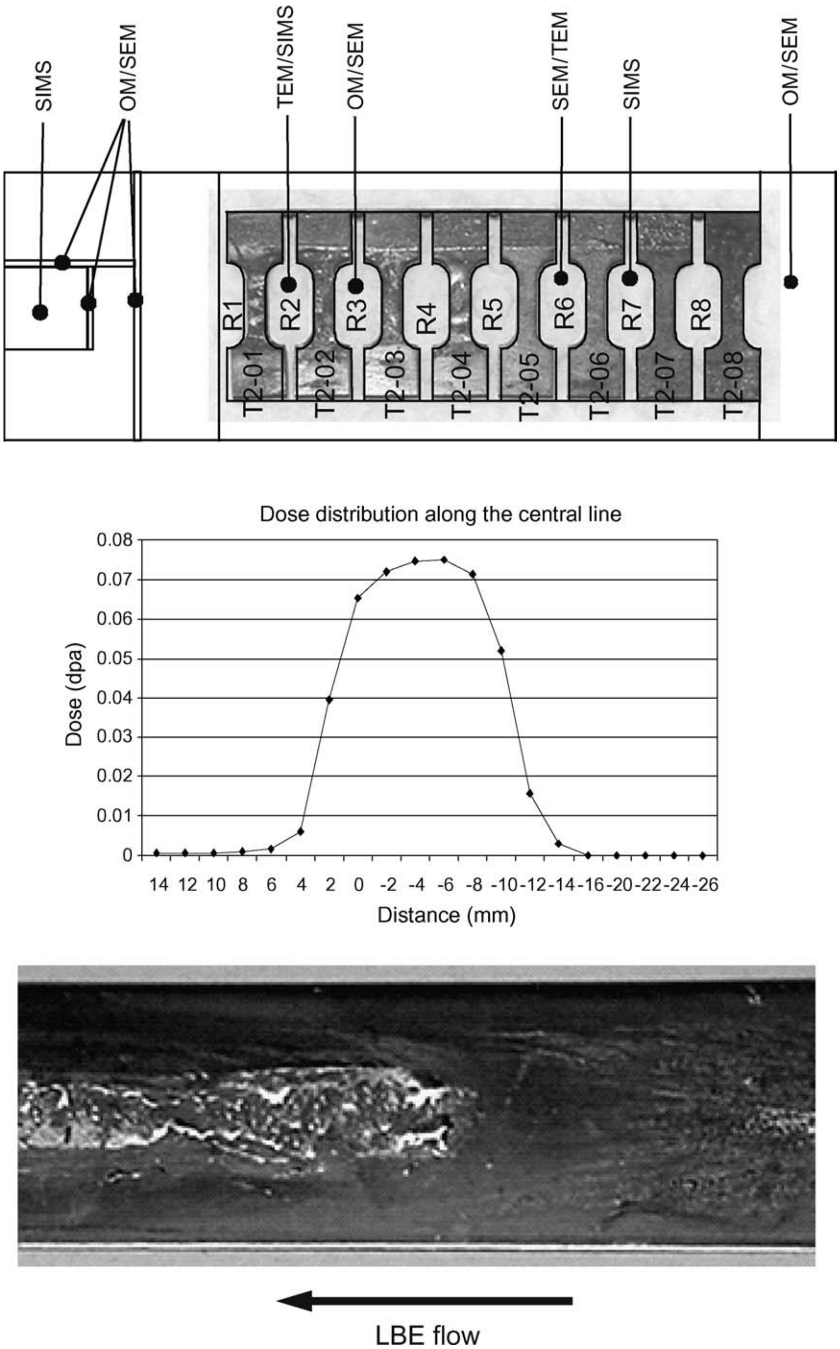

Fig. 1. A part of the ITS-specimen of LiSoR-2 (lower), the irradiation dose distribution calculated from the results of γ-scan along the central line of the ITS-specimen (middle), the sample cutting plan and the tensile samples cut from the ITS-specimen (upper). The LBE flow direction is indicated at the bottom.

consequence, the tension stress oscillated also with the proton beam. In the cases of LiSoR-3 and LiSoR-4, the thermal stresses were low and no plastic deformation could be produced. However, in LiSoR-2, the thermal stresses were high enough to cause localized fatigue deformation in the irradiation zones of both the TS-tube and ITS-specimen during irradiation.

After irradiation, the test sections were transported from Injector-I to the PSI Hotlab and dismantled in a hot-cell. For LiSoR-2, γ-mapping was performed on the ITS-specimen to identify the irradiation dose distribution in the irradiation zone. Afterwards, tensile samples of $14 \times 4 \times 1$ mm with a gauge section of $4 \times 1.5 \times 1$ mm were cut out from the region including the irradiation zone with an electron-discharge-machine (EDM). The small pieces between the tensile samples were used for microstructural and surface analyses. Fig. 1 shows a part of the ITS-specimen (lower), the irradiation dose distribution along the central line calculated from the γ-mapping result (middle), the sample cutting plan and the tensile samples obtained (upper). The LiSoR-3 and LiSoR-4 samples were cut out of both TS-tubes and ITS-specimens and the cutting plan was slightly different from that of LiSoR-2 [5].

Tensile tests with strain rates between 10^{-3} and $10^{-5}\,s^{-1}$ were performed at 300 °C in both Ar (+2% H) gas and LBE. The oxygen content in the LBE was saturated at 300 °C, which should be less than 1 wt-ppm. The details of the tensile tests are described elsewhere [8].

TEM samples of 1 mm in diameter were used for microstructural investigations. The observation was performed in a JEOL 2010 type transmission electron microscope operated at 200 kV. The most often used image conditions were bright field (BF) and weak beam dark field (WBDF) at g ($5g$–$6g$), $g = 200$ near $=011$.

3. Results and discussion

3.1. Tensile tests in Ar gas

The tensile tests were firstly carried out in Ar gas at a strain rate of $10^{-3}\,s^{-1}$. However, as it was indicated by the tensile tests performed on unirradiated samples in LBE that the LBE embrittlement phenomenon became more evident at a lower strain rate of $10^{-5}\,s^{-1}$ (see Section 3.2), the strain rate of most of the tests was $10^{-5}\,s^{-1}$.

Part of the samples cut from the ITS-specimen of LiSoR-2 and all of samples of LiSoR-3 were tested in Ar.

Fig. 2 shows the tensile curves of three LiSoR-2 samples (T2-02, -04 and -08) tested at strain rates of 10^{-3} and $10^{-5}\,s^{-1}$ in Ar. As shown in Fig. 1, sample T2-08 was cut from the outside of the irradiation zone and, therefore, was unirradiated. Sample T2-02 located in the irradiation zone and the irradiation temperature was about 470 °C (averaged). Sample T2-04 located at the edge of the irradiation zone with a large temperature variation, from about 320 °C to about 390 °C, cross the width. Due to the high irradiation temperature T2-02 does not show any radiation hardening (increase of yield strength). T2-04 indicates a slight hardening which can be attributed to its lower irradiation temperature at which radiation hardening usually takes place in martensitic steels [9].

The results of LiSoR-3 are presented in Fig. 3. In the ITS-specimen the irradiation temperature was $\leqslant$340 °C. Therefore, radiation hardening is expected. The results indicate that the hardening increases with increasing irradiation dose. For the TS-tube, the results show much less (<50%) hardening as compared to that of the ITS-specimen. It is believed to be due to its irradiation temperature was close to 400 °C or higher.

Accompany with the little radiation hardening, the ductility of irradiated samples slightly reduces, which suggests embrittlement induced by irradiation. The reduction increases somewhat with increasing irradiation dose. However, the reduction

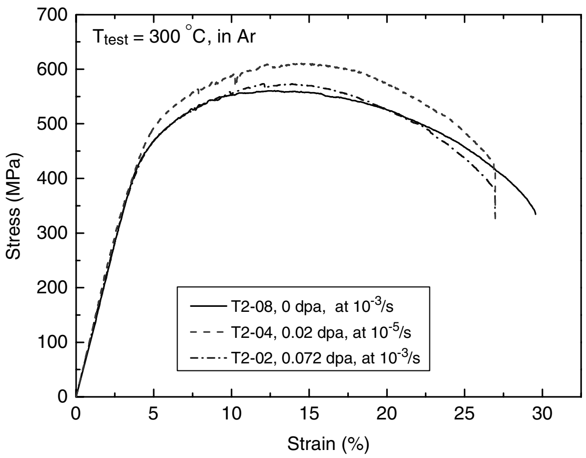

Fig. 2. Tensile curves of three samples, T2-02, -04 and -08, tested at 300 °C in Ar at strain rates of 10^{-3} and $10^{-5}\,s^{-1}$.

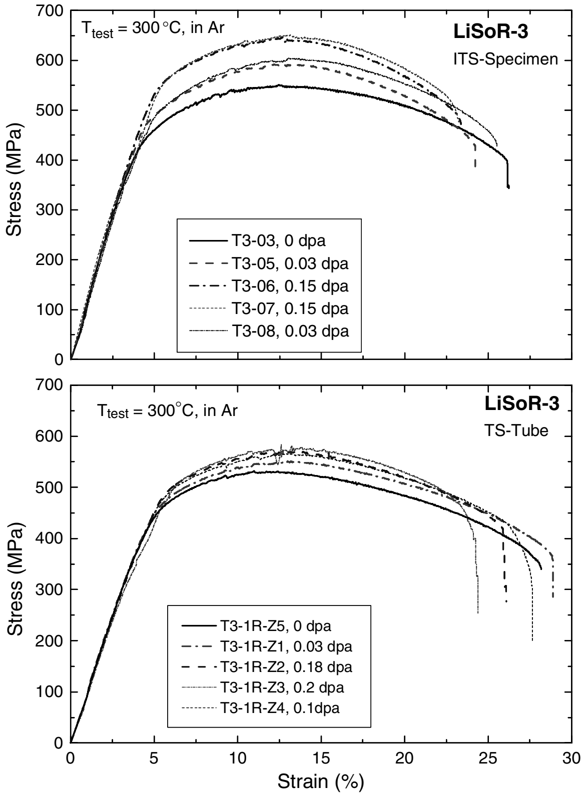

Fig. 3. Tensile curves of samples from the ITS-specimen (upper) and TS-tube (lower) of LiSoR-3 tested at 300 °C in Ar at strain rate of 10^{-5} s^{-1}.

is very little at such a low dose level, and not evident enough to reveal any LBE induced synergistic embrittlement effects as observed in the tests performed on martensitic steels in LBE [8].

The irradiation conditions of LiSoR-3 are similar to that of the beam window of the MEGAPIE target, with even higher stresses in the ITS-specimen. The results demonstrate that the mechanical properties of the T91 steel are only slightly degraded after irradiation to 0.2 dpa under the LiSoR irradiation condition, which implies that the beam window of the MEGAPIE target should not encounter any hazard at least during a short irradiation period of 2–3 weeks to reach an equivalent dose.

3.2. Tensile tests in LBE

In order to investigate the behaviour of irradiated samples when they are tested inside LBE, the rest of LiSoR-2 samples and most of LiSoR-4 samples were tested in LBE at 300 °C.

To find a proper testing condition in which the LBE embrittlement effects are relatively pronounced, different strain rates have been applied. Fig. 4 presents the tensile curves of unirradiated samples from the ITS-specimen of LiSoR-2 tested at three strain rates, 10^{-3}, 3.3×10^{-5} and 10^{-5} s^{-1}. The results show a clear tendency that the embrittlement effects become more pronounced at a lower strain rate. However, due to the limitation of the testing machine, 10^{-5} s^{-1} is almost the lowest available strain rate. Therefore, it was used for most of tests in LBE.

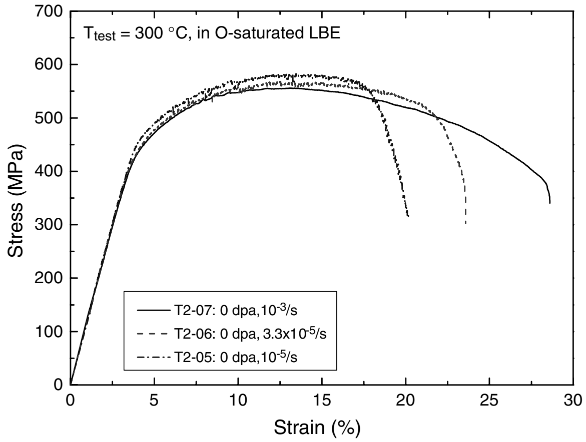

Fig. 4. Tensile curves of three samples, T2-05, -06 and -07, tested at 300 °C in oxygen-saturated LBE at strain rates of 10^{-3}, 3.3×10^{-5} and 10^{-5} s^{-1}.

Fig. 5 shows the results of tensile tests on three samples from the ITS-specimen of LiSoR-2 tested at 300 °C in LBE. Due to the same reason of samples T2-02 and -04 (Fig. 2), sample T2-03 does not indicate any radiation hardening, while T2-01 shows slight hardening even at a lower dose level. The embrittlement effect of LBE is clearly demonstrated

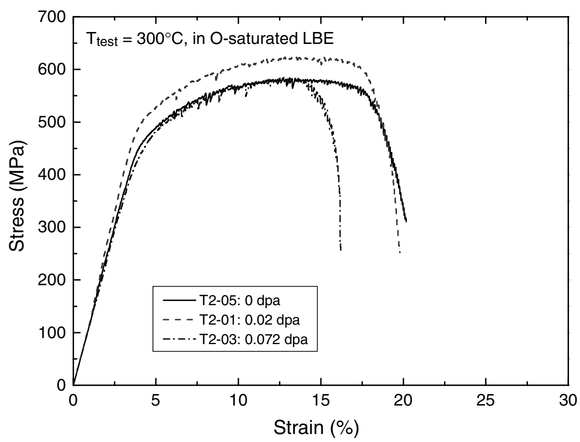

Fig. 5. Tensile curves of three samples, T2-01, -03 and -05, tested at 300 °C in oxygen-saturated LBE at strain rate of 10^{-5} s^{-1}.

by the significant reduction in the total elongations of all the three samples.

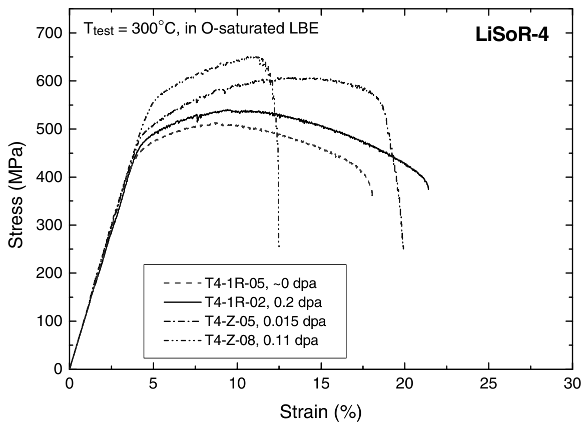

Fig. 6. Tensile curves of four samples of LiSoR-4 tested at 300 °C in oxygen-saturated LBE at a strain rate of 10^{-5} s^{-1}.

Fig. 7. Micrographs showing microstructure in unirradiated materials of (a) the TS-tube and (b) the ITS-specimen of LiSoR-2.

Only limited samples of LiSoR-4 have been tested. Fig. 6 presents the results of four samples, T4-1R-02 and T4-1R-05 from the TS-tube and T4-Z-05 and T4-Z-08 from the ITS-specimen. Similar to the samples of LiSoR-3, T4-1R-02 from the TS-tube is just slightly hardened, but T4-Z-08 from the ITS-specimen illustrates a significant hardening. Again, the results of all four samples clearly indicate LBE embrittlement effect by the decrease of total elongation as compared to that of samples (Fig. 3) tested in Ar.

As demonstrated by bending tests on irradiated T91 samples in LBE, the reduction of fracture toughness attributed to LBE effects increases with irradiation dose [10]. However, from the results presented in Figs. 5 and 6, it is difficult to see a clear irradiation dose dependence of LBE embrittlement. This is mainly due to the fact that many higher dose samples are irradiated at high temperatures and do not show radiation hardening which is believed to promote the embrittlement of martensitic steels in LBE [10]. This

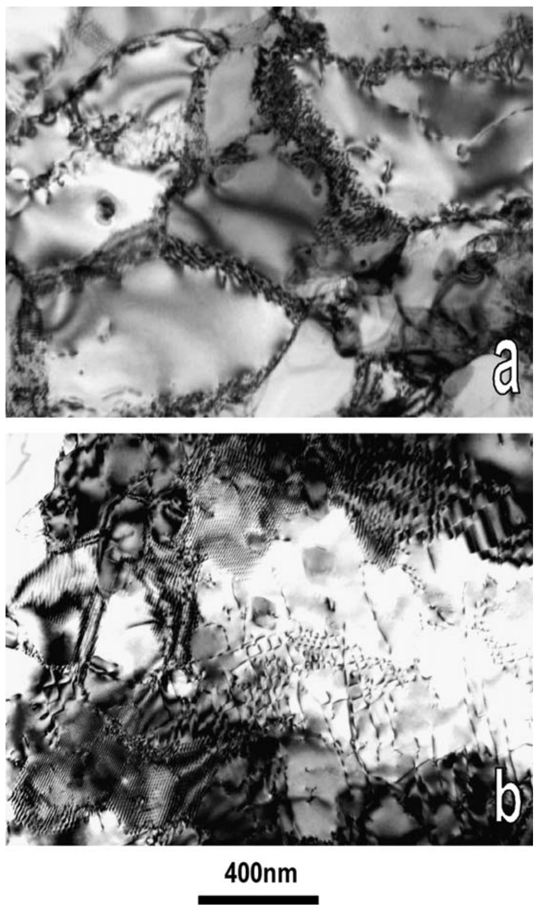

Fig. 8. Micrographs showing microstructure in irradiated materials of (a) the TS-tube and (b) the ITS-specimen of LiSoR-2.

fact is evident in sample T4-Z-08 which has the greatest radiation hardening and shows the most significant embrittlement case. Furthermore, the appearance of the LBE embrittlement phenomena likely depends on many parameters such as the testing temperature, the strain rate of deformation, the surface condition of samples, and the oxygen content in LBE etc. In the present case, the random microcracks on the transverse surfaces of the samples induced by EDM cutting should also give somewhat uncertainty of embrittlement level as observed in [8].

3.3. TEM observation

TEM observations were performed to investigate the microstructure in samples from both irradiated and unirradiated zones of the TS-tubes and ITS-specimens.

Fig. 7 illustrates the microstructure in unirradiated materials of the TS-tube and ITS-specimen of LiSoR-2. The graphs indicate typical martensitic structure in both steels used for the TS-tubes and ITS-specimens.

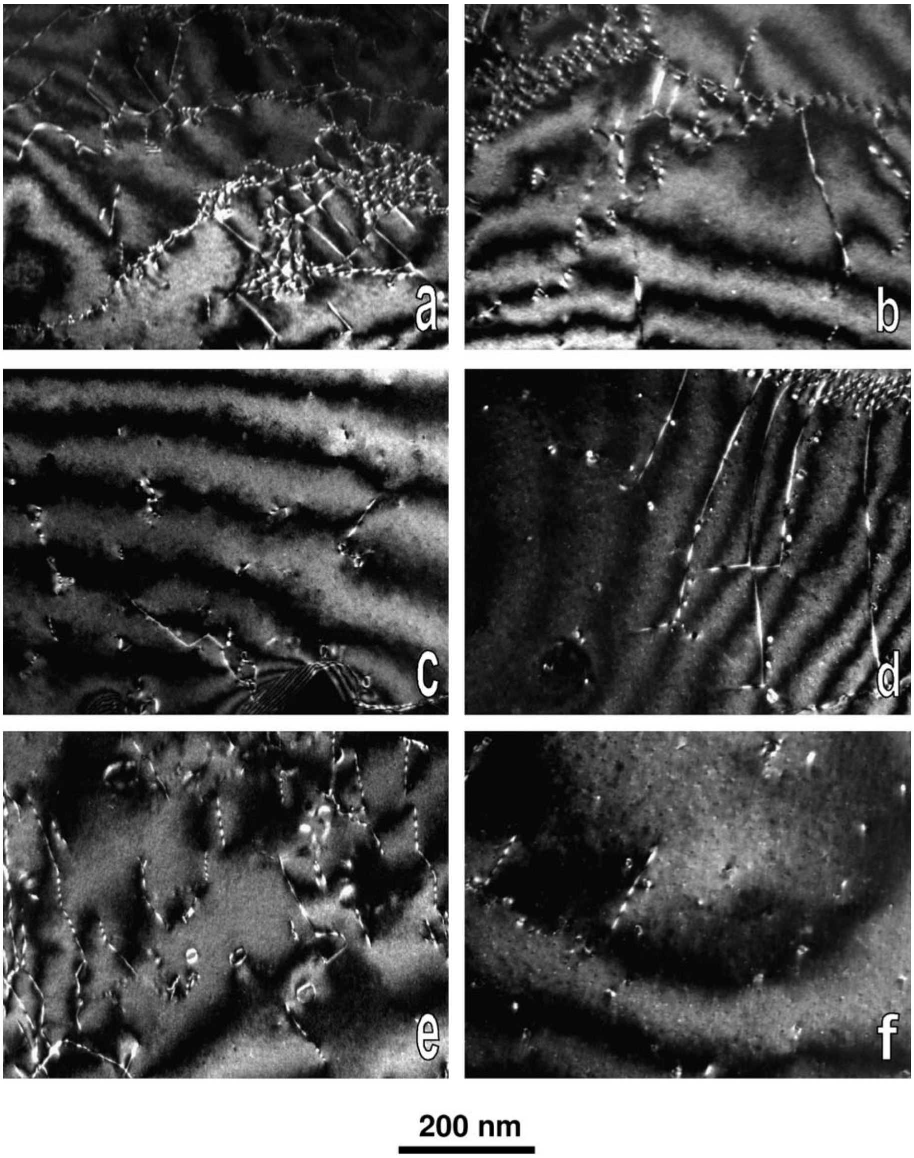

Fig. 9. Weak-beam-dark-field images showing microstructure in irradiated materials. (a), (c) and (e) are for the TS-tubes of LiSoR-2 to -4; and (b), (d) and (f) are for the ITS-specimen of LiSoR-2 to -4, respectively.

Due to high irradiation temperature and high stress (Table 1) the materials in the irradiation zones of the TS-tube and ITS-specimen of LiSoR-2 were deformed, which resulted in the crack in the TS-tube. This is demonstrated by the dislocation structure shown in Fig. 8. Well developed dislocation cells shown in Fig. 8(a) clearly indicate the heavy deformation in the irradiation zone of the TS-tube. In the ITS-specimen case, the dislocation cells seem less developed (Fig. 8(b)). However, the dislocation structure still suggests a very high deformation level.

The changes in dislocation structure of martensitic steels induced by irradiation can be characterized as the production of small defect clusters (black-dots as normally referred) and/or small dislocation loops, as shown in, e.g., [11]. The general observation is that both small defect clusters and loops are produced at lower temperatures (<350 °C). With increasing irradiation temperature to ~400 °C and above, small defect clusters disappear gradually and only loops and dislocation network are observed. The present TEM results agree with the general observation.

In the TS-tube of LiSoR-2, as shown in Fig. 9(a), the general features are dislocation networks and/or dislocation tangles. Small defect clusters and loops were hardly observed. In the TS-tube of LiSoR-3 and -4 as one can see from Fig. 9(c) and (e), respectively, some dislocation loops appear in relatively low density though the main feature is dislocation tangles. In the Lsor-3 case, some small clusters can be also seen. The results suggest that the irradiation temperatures for the three TS-tubes are in an order as given in Table 1: LiSoR-2 is the highest, followed by LiSoR-4, and LiSoR-3 is the lowest. Furthermore, it suggests that the temperatures of the TS-tubes of LiSoR-2 and -4 should be close to 400 °C or above, and that of LiSoR-3 TS-tube must be below 400 °C.

As compared to the situation in the TS-tubes, the main difference in the ITS-specimens is that more loops and defect clusters are observed. In the ITS-specimen of LiSoR-2, few loops and small defect clusters are unexpectedly detected (Fig. 9(b)). The reason is not clear. In the ITS-specimens of LiSoR-3 and -4, not only some loops but also high-density very small defect clusters (<2 nm) were seen (Fig. 9(d) and (f)). This means that the irradiation temperatures of the ITS-specimens were certainly lower than 400 °C.

Although no quantitative results have been evaluated, the above TEM results agree qualitatively with the tensile testing results, namely where more defect clusters and loops are observed show higher radiation hardening.

4. Conclusions

Tensile tests in both Ar and LBE environments and TEM observations were performed on the samples cut from the TS-tubes and ITS-specimens of LiSoR-2 to -4. The main results are:

1. No obvious synergetic embrittlement effects of LBE were observed in the T91 steel under the LiSoR irradiation condition up to a dose of 0.2 dpa.
2. LBE embrittlement took place when the samples were tensile tested in LBE, which could be attributed to the micro-cracks induced by EDM cutting.
3. Irradiation produced small defect clusters and loops were observed in the ITS-specimens of LiSoR-3 and LiSoR-4. The main features of the dislocation structure in the ITS-specimen of LiSoR-2 and the TS-tubes are dislocation tangles and dislocation networks. The TEM results support the tensile test results and also fairly reflect the calculated irradiation temperatures.

References

[1] G.S. Bauer, M. Salvatores, G. Heusener, J. Nucl. Mater. 296 (2001) 17.
[2] T. Kirchner et al., J. Nucl. Mater. 318 (2003) 70.
[3] H. Glasbrenner, V. Boutellier, Y. Dai, S. Dementjev, F. Gröschel, L. Ni, D. Viol, T. Kirchner, Technical Report, PSI, TM-34-02-04, November 2002.
[4] Y. Dai, H. Glasbrenner, V. Boutellier, R. Bruetsch, X. Jia, F. Groeschel, J. Nucl. Mater. 335 (2004) 232.
[5] H. Glasbrenner, R. Brütsch, Y. Dai, F. Gröschel, M. Martin, J. Nucl. Mater., these Proceedings, doi:10.1016/j.jnucmat.2006.05.040.
[6] K. Samec, Temperature calculations of the LiSoR experiment, PSI Technical Report, TM-34-05-02, 2005.
[7] Y. Dai, B. Oliver, A comparison between calculated and measured He and H contents of STIP samples, in press.
[8] Y. Dai, B. Long, F. Groeschel, J. Nucl. Mater., these Proceedings, doi:10.1016/j.jnucmat.2006.05.039.
[9] M.I. deVries, in: A.S. Kumar, D.S. Gelles, R.K. Nanstad, E.A. Little (Eds.), Effects of Radiation on Materials: 16th International Symposium, ASTM STP 1175, ASTM, Philadelphia, 1993, p. 558.
[10] Y. Dai, J. Henry, T. Auger, J.-B. Vogt, A. Almazouzi, H. Glasbrenner, F. Groeschel, J. Nucl. Mater., these Proceedings, doi:10.1016/j.jnucmat.2006.05.036.
[11] X. Jia, Y. Dai, J. Nucl. Mater. 318 (2003) 207.